

# Wafer Bonded Capacitive Micromachined Underwater Transducers

Selim Olcum,<sup>1,\*</sup> Kagan Oğuz,<sup>1</sup> Muhammed N. Şenlik,<sup>1</sup> F. Yalçın Yamaner,<sup>2</sup>  
Ayhan Bozkurt,<sup>2</sup> Abdullah Atalar,<sup>1</sup> Hayrettin Köymen,<sup>1</sup>

<sup>1</sup> Bilkent University, Electrical & Electronics Engineering Department, Ankara, 06800 TURKEY

<sup>2</sup> Sabancı University, Faculty of Engineering & Natural Sciences, İstanbul, 34956 TURKEY

\* selim@ee.bilkent.edu.tr

**Abstract** — In this work we have designed, fabricated and tested CMUTs as underwater transducers. Single CMUT membranes with three different radii and 380 microns of thickness are fabricated for the demonstration of an underwater CMUT element. The active area of the transducer is fabricated on top of a 3" silicon wafer. The silicon wafer is bonded to a gold electrode coated glass substrate wafer 10 cm in diameter. Thermally grown silicon oxide layer is used as the insulation layer between membrane and substrate electrodes. Electrical contacts and insulation are made by epoxy layers. Single CMUT elements are tested in air and in water. Approximately 40% bandwidth is achieved around 25 KHz with a single underwater CMUT cell. Radiated pressure field due to second harmonic generation when the CMUTs are driven with high sinusoidal voltages is measured.

**Keywords-component; Capacitive Micromachined Ultrasonic Transducers, underwater transducers, anodic bonding, second harmonic generation.**

## I. INTRODUCTION

Capacitive micromachined ultrasonic transducers (CMUT) have been under investigation for almost 15 years. Many fabrication technologies are proposed based on sacrificial layer process or wafer bonding process in order to fabricate efficient ultrasonic transducers. Applications such as medical imaging, high intensity focussed ultrasound, intravascular ultrasound, airborne acoustics, microphones and nondestructive evaluation attracted attention for possible use of CMUTs. The operational frequency range in focus has been mainly between 1 MHz to 30 MHz. Recently, potential of achieving a large bandwidth and high efficiency from CMUTs attracted more applications at lower frequency bands. Recent studies show that airborne CMUTs can achieve a high transduction efficiency and bandwidth around 50 KHz [1].

Acoustical energy has been used underwater in several areas ranging from commercial, scientific and military areas. In lower frequency range (1 kHz – 100 kHz), acoustical systems are utilized underwater and on surface platform applications, i.e., navigation systems, active and passive sonar transducers, seismic and environmental observation systems. In the higher frequency range the applications are more limited due to the higher attenuation and noise underwater. Such applications are restricted in short ranges. Most common practices are purse

TABLE I. PHYSICAL PARAMETERS OF THE CMUT CELLS

	$t_m$ ( $\mu\text{m}$ )	$f_r$ (kHz)	$a$ (mm)	$t_g$ ( $\mu\text{m}$ )	$t_i$ ( $\mu\text{m}$ )
A	380	84.9	4	4-4.5	0.5
B	380	54.8	5	4-4.5	0.5
C	380	38.2	6	4-4.5	0.5

seining, Doppler sonars and underwater imaging systems.

Achieving a high acoustical power during the transmit cycle and a high sensitivity during the receive cycle in a large bandwidth is difficult. In the case of building an array of transducers, building transmit and receive elements along with the required interconnects to the dedicated transmit and receive circuitry is another challenge. For low frequency applications production of thin transducers is also a difficult task.

It's been demonstrated that CMUTs offer excellent properties such as wide bandwidth [2], ease of array fabrication and integrating the dedicated electronics along with the transducers, [3] thanks to the microfabrication techniques utilized during fabrication. Recent studies show that high power outputs can be obtained [4] and high receive sensitivities can be achieved using CMUTs [2]. CMUT's large bandwidth, high sensitivity, low cost fabrication and ease of integration with electronics make it a good candidate for an underwater transducer. However, extra care should be exercised in order to utilize the full merit of the CMUTs. Especially, nonlinear behavior during transmit mode should be taken into account.

In this work we have designed, fabricated and tested CMUTs as underwater transducers. Single CMUT membranes with three different radii and 380  $\mu\text{m}$  of thickness are fabricated for the demonstration of an underwater CMUT cell. The results of the underwater measurements are reported and compared with those obtained from an equivalent circuit model.

## II. DESIGNING AN UNDERWATER TRANSDUCER

In principle, CMUTs work with a fixed DC bias generating a static force deflecting the membrane. Therefore, any external static force changes the operating point of the device. Underwater hydrostatic pressure affects the operation of the CMUT membranes. In this study, we limit ourselves to the

This work is supported by TUBITAK under the grants 105E023 and 107T921.

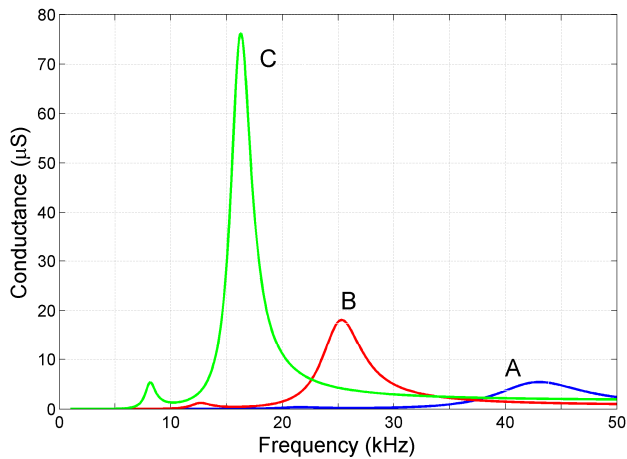


Figure 1. Calculated conductances of cells A, B and C in water for 100 V<sub>pp</sub> applied with 50 V DC bias. Calculations are made using the equivalent circuit developed in [5].

design CMUTs operating at a depth of 0-2 m. We have designed three different sized CMUT cells (A, B and C) for operation underwater. The gap height of the transducers is chosen in order to achieve a reasonable operating voltage under 250V for cell B. A highly doped, low resistivity silicon wafer is used as the membrane. A thermally grown silicon oxide layer is used as the insulation layer between top and bottom electrodes of the CMUT. The insulation layer should be thick enough, in order to prevent an electrical breakdown. The dielectric strength of the thermally grown oxide is typically 800–1000 V/μm. The thickness of the isolation layer is chosen to be 500 nm in order to maintain 250 V of operation voltage. The physical parameters of the designed CMUT cells can be seen in Table 1, where  $t_m$  is the thickness,  $f_r$  is the airborne resonance frequency and  $a$  is the radius of the membrane. In addition,  $t_i$  is the insulation layer thickness and  $t_g$  is the gap height of the designed CMUT cells.

The conductance graphs of the single cell CMUTs are calculated using the equivalent circuit model developed in [5]. Each cell is simulated by applying 100 V<sub>pp</sub> sinusoid on 50 V DC bias. The conductance curves are calculated by taking the ratio of the current and voltage of the driving source. In addition to the single cell CMUTs, we have designed an array consisting of B type cells. We have packed a total of 26 cells on a 3" silicon wafer.

### III. FABRICATION

For the fabrication of the underwater CMUT transducer, we have utilized anodic wafer bonding technology. Anodic bonding is used to bond a silicon wafer to a borosilicate wafer using proper pressure, electric field and temperature. The borosilicate wafer has mobile ions at the bonding temperature in order to maintain the migration of ions and formation of a depletion layer at the interface. In this work we have used commercially available Borofloat wafers.

A highly doped, double side polished silicon wafer is used at the membrane side. The thickness of the wafer determines the thickness of the membrane which is 380 μm in this case (Fig. 2a). First, the CMUT cavity gap of 4.5 μm is etched using a reactive ion etching (RIE) reactor (Fig. 2b). A 250 nm of

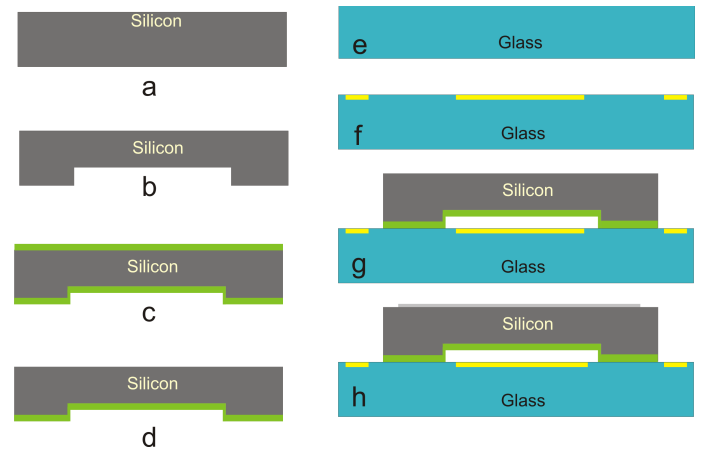


Figure 2. Microfabrication process steps of CMUT cells.

chromium layer is used as the etch mask in the RIE. For passivation of the silicon surface 500 nm of silicon oxide is thermally grown in a diffusion furnace. The silicon wafer is kept in the furnace at 1050°C for about an hour in the presence of adequate water vapor (Fig. 2c). The silicon oxide at the back side of the silicon wafer is etched using the RIE reactor (Fig. 2d).

Having completed the membrane side, the substrate side is fabricated on a 3.2 mm thick borosilicate wafer (Fig. 2e). This wafer is chosen to be quite thick in order to maintain a rigid substrate. Since the smoothness of the borosilicate surface is critical for the success of the anodic bonding, the substrate electrode is buried on the glass wafer (Fig. 2f). An image reversal photoresist (AZ5214E) is patterned for the lift off process. Before the evaporation of the gold electrode, the glass is etched approximately by the thickness of gold to be evaporated. As the substrate electrode, 5 nm of chromium and 45 nm of gold are deposited by thermal evaporation. The borosilicate and silicon wafers are cleaned at 120°C in Piranha etch (1:3 H<sub>2</sub>O<sub>2</sub>:H<sub>2</sub>SO<sub>4</sub>) for 15 minutes.

The prepared wafers are then bonded using anodic bonding option of EVG 501 Universal Bonder (Fig. 2g). The process has been performed at 450°C at an ambient pressure of 0.1 μbar. When the bonding voltage is applied between the wafers, it's observed that a peak current at the order of tens of milliamperes is drawn from the power supply. The drawn current exponentially decays within the next few minutes. This peak current indicates that the borosilicate wafer has a high conductance initially. Therefore, in the first few seconds the bonding voltage is applied effectively across the silicon oxide isolation layer. This high potential may cause the thin oxide layer to breakdown during the bonding. Hence, the bonding voltage is increased in small steps in order to protect the oxide layer from the breakdown. Using this stepping method we were able to apply a bonding voltage as high as 1000 V. The bonding process has been started from 200 V and the bond voltage is increased with 100 V steps every 10 minutes.

Since the borosilicate wafer is larger than the silicon wafer, the substrate electrical contacts are taken from the exposed surface of the borosilicate wafer. For the top electrode of the CMUT, an aluminum layer is evaporated on top of the silicon membrane after the bonding process (Fig. 2h).

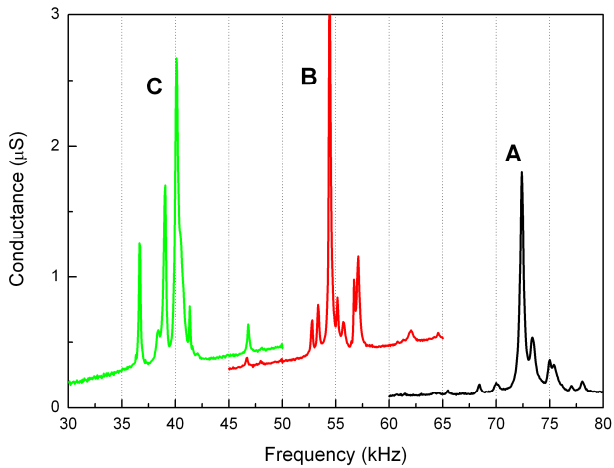


Figure 3. Conductance graphs of airborne A, B and C cells measured by an impedance analyzer. 1V<sub>pp</sub> is applied on 40V of DC bias.

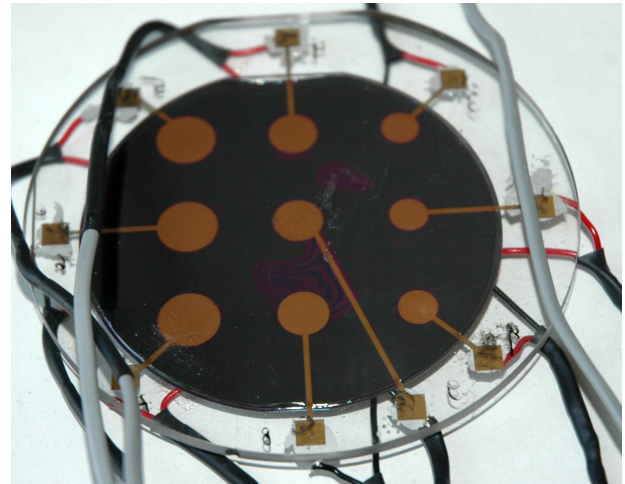


Figure 4. A photograph of fabricated CMUTs cells A, B and C, 3 each.

Although anodic bonding is a mature technology and already used in a large variety of industrial products, there are still several aspects which should be investigated [7]. It has been mentioned in the literature that suspended structures tend to stick to the glass wafer due to the applied bonding voltage. In the case of CMUTs, collapse of the membrane is prevented by increasing the bonding voltage in steps smaller than the collapse voltage. Using incremental bond voltages and thin metal layers improved the bonding area and quality. However, achieving a 100% successful bond is still problematic when the gold electrode area is large. Process optimization of the anodic bonding step is still in progress for the array of CMUT cells.

Having completed the microfabrication process steps in cleanroom, electrical contacts to the electrodes are made using a commercially available silver conductive epoxy Eccobond 83C (Emmerson-Cumming). The transducers are mounted in a slightly larger holder using Eccobond 45 epoxy (Emmerson Cumming). An equal sized 2 mm thick rigid foam disk (Rohacell) is fixed at the backside. This way the transducer is terminated by a low impedance medium at the backside. After the curing, the exposed region of the aluminum electrode, which is the active area of the transducer is painted in order to achieve electrical insulation for immersion experiments.

#### IV. MEASUREMENTS

The fabricated transducers are first tested in air. The conductance and susceptance of the transducers are measured by an impedance analyzer (HP4194A). The measurements are made with 40 V of bias and 1 V<sub>pp</sub> of AC voltage. The conductances of cells A, B and C are shown in Fig. 3.

Underwater performances of the CMUT cells are tested in our open water testing facility on Bilkent University Lake. CMUTs are driven with multiple cycle bursts of sinusoids amplified by a power amplifier. The signal generated from the signal source (SRS DS345) is amplified 10 times by a power amplifier (Krohn-Hite 7500). The amplitude of the applied signal is kept at 100 V<sub>pp</sub>. A 50 V DC bias voltage is applied in order to keep the excitation unipolar. The radiated acoustical

energy is detected by a calibrated hydrophone (Neptune D70H).

The frequency response of CMUT cells has been determined by use of testing software running on LabView. The hydrophone is kept at approximately 1 m away from the radiating CMUTs. The received signal is corrected with the calibration data of the hydrophone. The resulting absolute pressure spectra of the CMUTs at 1 m are depicted in Fig. 5. The results are not compensated for the diffraction loss. The differences at the peak pressures of different CMUTs can be attributed to differences in collapse voltages. Approximately, a 40% bandwidth is achieved from the cell type B.

Similarly, an array of type B cells has been tested both in air and underwater. Airborne impedance measurements indicate too many unaccounted resonances due to poor bonding. Nevertheless, we were able to achieve 300 Pa<sub>rms</sub> pressure underwater at 1 m away from the CMUTs with a 100 V<sub>pp</sub> excitation.

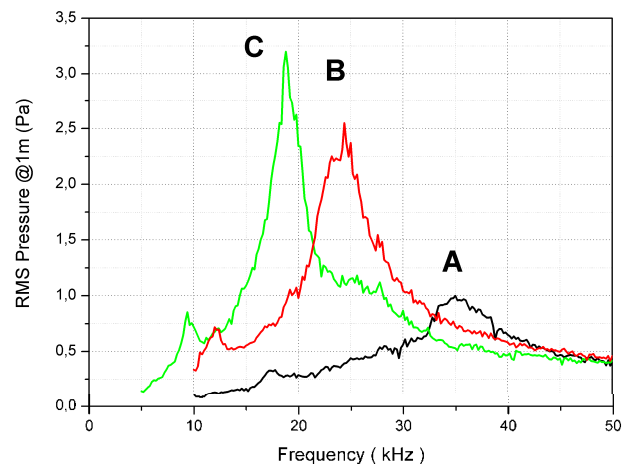


Figure 5. RMS pressure generated by cells A, B and C measured at 1 m away from the CMUT surfaces by a calibrated hydrophone with 100V<sub>pp</sub> on 50 V DC bias.

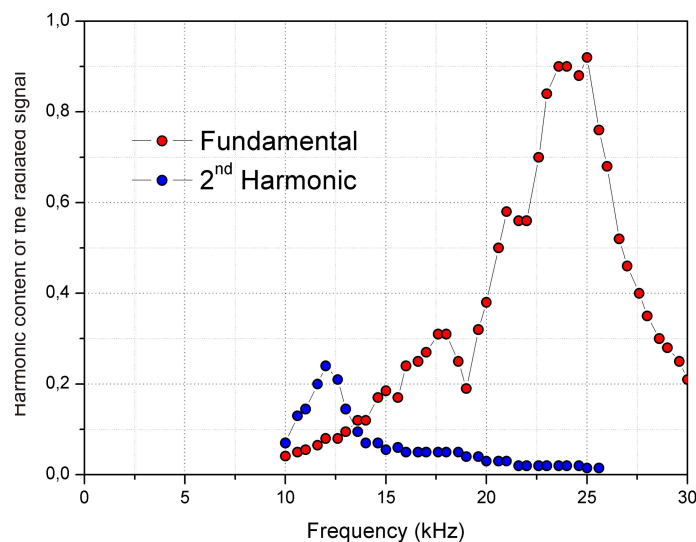
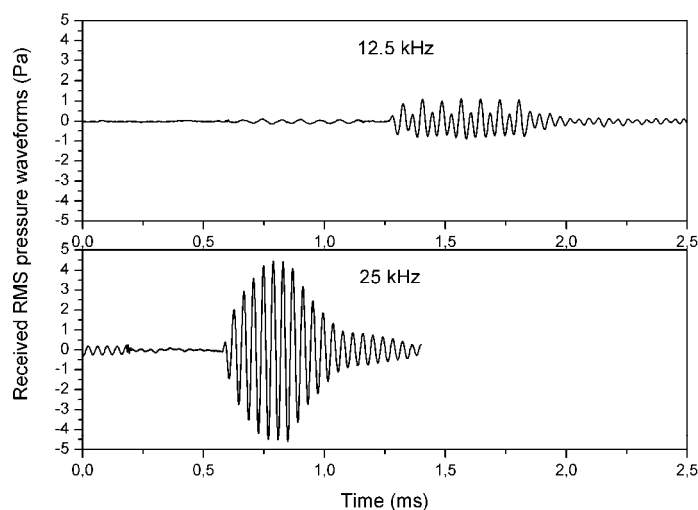


Figure 7. Harmonic content of each of the detected pressure waveforms by the hydrophone for cell B is driven by 100 V<sub>pp</sub> on 50 V bias.

## V. DISCUSSION & CONCLUSIONS

During the immersion experiments of cells A, B and C, we have observed small peaks at the half of resonance frequency as seen in Fig. 5. These peaks are attributed to nonlinear behavior of CMUTs. The recorded pressure waveforms are depicted in Fig. 6 for the cell B at 12.5 kHz and 25 kHz. As can be seen in the waveforms, the radiation in the case of 12.5 kHz excitation has a strong component at 25 kHz. That is because the second harmonic of the 12.5 kHz excitation coincides with the resonance frequency of the cell. In Fig. 7, we show the amount of fundamental and second harmonic components at different frequencies. The second harmonic component becomes significant only when that frequency is around the resonance of the cell. These small peaks at half the resonance are also observed in our equivalent circuit simulations results shown in Fig. 1.

In this work, we have fabricated and tested underwater CMUT transducers. The radiation impedance seen by a single cell is lower than that seen by an array of CMUT cells [7]. Therefore, the bandwidth of an underwater CMUT array would be larger than the bandwidths presented in this paper. It has been demonstrated that operation of CMUTs as underwater acoustic transducers is possible and needs further investigation for optimal use.

## ACKNOWLEDGMENTS

S.O. acknowledges the support of TUBITAK and ASELSAN for their Ph.D. Scholarship Programs. A.A. acknowledges the support of TUBA. We gratefully acknowledge the support of METU-MET for the anodic bonding tool. We thank Sinan Taşdelen for his generous help during the epoxy sealing process and Dr. Ebru Topalli for her kind assistance during the bonding process.

## REFERENCES

- [1] I. O. Wygant, M. Kupnik, J. C. Windsor, W. M. Wright, M. S. Wochner, G. G. Yaralioglu, M. F. Hamilton, and B. T. Khuri-Yakub, "50 kHz Capacitive Micromachined Ultrasonic Transducers for Generation of Highly Directional Sound with Parametric Arrays," *IEEE Transactions on Ultrasonics Ferroelectrics and Frequency Control*, vol. 56, pp. 193-203, Jan 2009.
- [2] R. O. Guldiken, J. Zahorian, F. Y. Yamaner, and F. L. Degertekin, "Dual-Electrode CMUT With Non-Uniform Membranes for High Electromechanical Coupling Coefficient and High Bandwidth Operation," *IEEE Transactions on Ultrasonics Ferroelectrics and Frequency Control*, vol. 56, pp. 1270-1276, Jun 2009.
- [3] I. O. Wygant, X. Zhuang, D. T. Yeh, O. Oralkan, A. S. Ergun, M. Karaman, and B. T. Khuri-Yakub, "Integration of 2D CMUT arrays with front-end electronics for volumetric ultrasound imaging," *IEEE Transactions on Ultrasonics Ferroelectrics and Frequency Control*, vol. 55, pp. 327-342, Feb 2008.
- [4] B. Bayram, O. Oralkan, A. S. Ergun, and E. Haeggstrom, "Capacitive micromachined ultrasonic transducer design for high power transmission," *IEEE Transactions on Ultrasonics Ferroelectrics and Frequency Control*, vol. 52, pp. 326-339, Feb 2005.
- [5] K. Oguz, S. Olcum, M.N. Senlik, V. Tas, A. Atalar, H. Koymen, "Nonlinear modelling of an immersed transmitting capacitance micromachined ultrasonic transducer for harmonic balance analysis," submitted for publication, *IEEE Transactions on Ultrasonics Ferroelectrics and Frequency Control*.
- [6] T. Rogers, N. Aitken, K. Stribley, and J. Boyd, "Improvements in MEMS gyroscope production as a result of using in situ, aligned, current-limited anodic bonding," *Sensors and Actuators a-Physical*, vol. 123-24, pp. 106-110, Sep 23 2005.
- [7] M.N. Senlik, S. Olcum, H. Koymen and A. Atalar, "Radiation impedance of an array of circular capacitive micromachined ultrasonic transducers," submitted for publication, *IEEE Transactions on Ultrasonics Ferroelectrics and Frequency Control*.